Production of quarkonia states with the ATLAS detector

L. XU on behalf of the ATLAS COLLABORATION

Brookhaven National Laboratory - Upton, NY, USA

Summary. — A wide program of studies of heavy flavour production at the LHC is performed with the ATLAS detector, including charm and beauty hadrons, quarkonia production in both flavours, and associated production of $J/\psi + W$, $J/\psi + Z$ and $J/\psi + J/\psi$. This report will cover recent results, and discuss in particular the results on $X(3872)$ and $J/\psi + J/\psi$ production, based on the data collected at 8 TeV. For the $X(3872)$ production measurement, an enhancement in the non-prompt production at low p_T, and of a shorter effective lifetime, is observed. The enhancement might be related to the production of B_c state that decays inclusively to $X(3872)$. The differential $J/\psi + J/\psi$ cross-section is measured and the fraction of prompt pair events due to double parton scattering is determined by studying kinematic correlations. The total and double parton scattering cross-sections are compared with predictions.

1. – Introduction

The production mechanism of heavy quarkonium has been a long-standing and intriguing problem in Quantum Chromodynamics (QCD), since it involves both perturbative and non-perturbative QCD. Quarkonium production at the LHC offers an ideal system to test the production models and deepen our understanding of non-perturbative QCD. More recently, through novel studies of exclusive production models such as $J/\psi + J/\psi$ and $J/\psi + W/Z$, quarkonium can provide an interesting window into the study of multiple parton interactions (MPI), while also providing new observables for testing production predictions.

In this report we present recent quarkonia production measurements at 8 TeV, namely $\psi(2S)$ and $X(3872)$ production in $J/\psi\pi^+\pi^-$ final states, and prompt $J/\psi + J/\psi$ production. In all of these results, J/ψ mesons are reconstructed using the $J/\psi \to \mu^+\mu^-$ decay mode.

2. – $\psi(2S)$ and $X(3872)$ production measurements at 8 TeV

The hidden-charm state $X(3872)$ was discovered by the Belle Collaboration in 2003 [1] through its decay to $J/\psi\pi^+\pi^-$ in the exclusive decay $B^\pm \to K^\pm J/\psi\pi^+\pi^-$. Its existence was subsequently confirmed by many experiments [2-4]. A particularly interesting aspect of the $X(3872)$ is the closeness of its mass, 3871.69 ± 0.17 MeV [5], to the $D^0\bar{D}^{*0}$ threshold, such that it was hypothesised to be a $D^0\bar{D}^{*0}$ molecule [6]. A later interpretation of $X(3872)$ as a mixed $\chi_{c1}(2P)$–$D^0\bar{D}^{*0}$ state, where the $X(3872)$ is produced predominantly through its $\chi_{c1}(2P)$ component, was adopted in conjunction with the next-to-leading-order (NLO) NRQCD model and fitted to CMS data [7] with good agreement [8]. In this analysis [9], a measurement of the differential cross sections for the production of $\psi(2S)$ and $X(3872)$ states in the decay channel $J/\psi\pi^+\pi^-$ is performed, using 11.4 fb^{-1} of proton–proton collision data collected by the ATLAS experiment at the LHC at $\sqrt{s} = 8$ TeV.

The production cross sections of the $\psi(2S)$ and $X(3872)$ states are measured in bins of $J/\psi\pi^+\pi^-$ transverse momentum, from 10 to 70 GeV. In order to separate the prompt production of the $\psi(2S)$ and $X(3872)$ states from the non-prompt production occurring via the decays of long-lived particles such as b-hadrons, the data sample in each p_T bin is further divided into intervals of pseudo-proper lifetime τ. Two models of the lifetime dependence of the non-prompt production are considered: a model with a single effective lifetime, and an alternative model with two distinctly different effective lifetimes. The two models give compatible results for the prompt and non-prompt differential cross sections of the $\psi(2S)$ and $X(3872)$. Within the single-lifetime model, assuming that non-prompt $\psi(2S)$ and $X(3872)$ originate from the same mix of parent b-hadrons, the following result is obtained for the ratio of the branching fractions:

$$R_B^{1L} = \frac{\mathcal{B}(B \to X(3872) + \text{any})\mathcal{B}(X(3872) \to J/\psi\pi^+\pi^-)}{\mathcal{B}(B \to \psi(2S) + \text{any})\mathcal{B}(\psi(2S) \to J/\psi\pi^+\pi^-)}$$

(1)
$$= (3.95 \pm 0.32(\text{stat}) \pm 0.08(\text{sys})) \times 10^{-2}.$$

In the two-lifetime model, the two lifetimes are fixed to expected values for $X(3872)$ originating from the decays of B_c and from long-lived b-hadrons, respectively, with their relative weight determined from the fits to the data. The measured ratio of long-lived $X(3872)$ to long-lived $\psi(2S)$ is shown in fig. 2. The fraction of the short-lived non-prompt component in $X(3872)$ production, for $p_T > 10$ GeV, is found to be

(2) $$\frac{\sigma(pp \to B_c + \text{any})\mathcal{B}(B_c \to X(3872) + \text{any})}{\sigma(pp \to \text{non-prompt } X(3872) + \text{any})} = (25 \pm 13(\text{stat}) \pm 2(\text{sys}) \pm 5(\text{spin}))\%.$$

Since B_c production is only a small fraction of the inclusive beauty production, this value of the ratio would mean that the production of $X(3872)$ in B_c decays is strongly enhanced compared to its production in the decays of other b-hadrons.

The prompt $X(3872)$ cross-section measurement, as shown in fig. 1 (left), is found to be consistent with the predictions of the NLO NRQCD model, which considers $X(3872)$ to be a mixture of $\chi_{c1}(2P)$ and a $D^0\bar{D}^{*0}$ molecular state, with the production being dominated by the $\chi_{c1}(2P)$ component and the normalisation fixed through the fit to CMS data. The non-prompt production of $\psi(2S)$ is described by the FONLL predictions within the uncertainties. But the same predictions, recalculated for $X(3872)$ using the branching
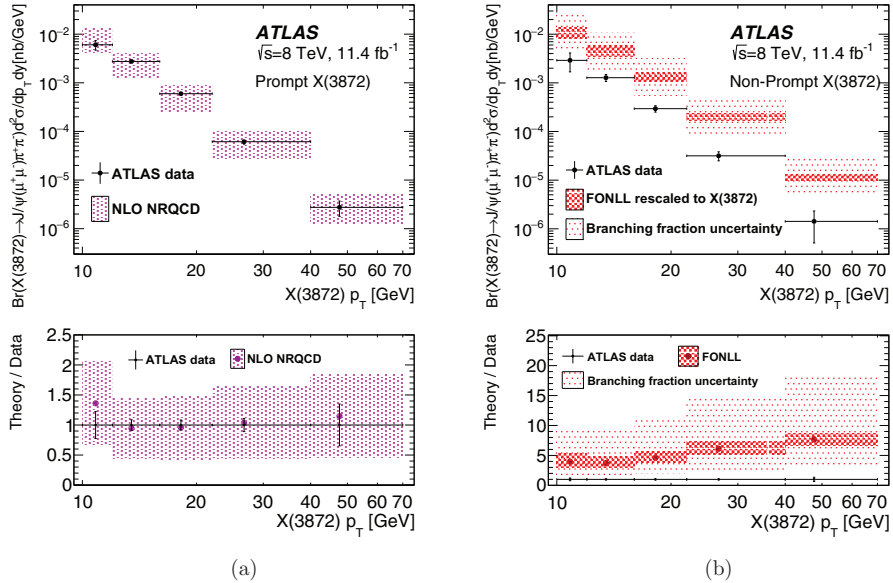
Fig. 1. – Measured cross section times branching fractions as a function of p_T for (a) prompt $X(3872)$ compared to NLO NRQCD predictions with the $X(3872)$ modelled as a mixture of $\chi_{c1}(2P)$ and a $D^0\bar{D}^{*0}$ molecular state [8], and (b) non-prompt $X(3872)$ compared to the FONLL [10] model prediction, recalculated using the branching fraction estimate from ref. [11] as described in the text.

fraction extracted from the Tevatron data, as shown in fig. 1 (right), overestimate the non-prompt production of $X(3872)$, especially at large transverse momenta. The non-prompt fraction of $X(3872)$ production is shown in fig. 2 (right). No sizeable dependence on p_T is observed and this measurement agrees within errors with the CMS result obtained at $\sqrt{s} = 7\,\mathrm{TeV}$ [7].

3. – Prompt J/ψ pair production measurements at 8 TeV

The study of the simultaneous production of two prompt J/ψ mesons offers an opportunity to test our understanding of non-perturbative QCD. These events are also sensitive to NLO and higher-order perturbative QCD corrections, in addition to providing an opportunity to study and compare J/ψ production models. Di-J/ψ events can be produced from a single gluon-gluon collision via single parton scattering (SPS) or from two independent parton-parton scatters in a single proton-proton collision, known as double parton scattering (DPS). In particular, the production of di-J/ψ events via double parton scattering presents a unique insight into the structure of the proton and allows a better comprehension of backgrounds to searches for new phenomena. A simplified ansatz for defining the DPS cross-section in terms of the production cross-sections of the two final states and an effective cross-section is described in ref. [12] as

$$(3) \qquad \sigma_{\mathrm{eff}} = \frac{1}{2}\frac{\sigma_{J/\psi}^2}{\sigma_{\mathrm{DPS}}^{J/\psi,J/\psi}} = \frac{1}{2}\frac{\sigma_{J/\psi}^2}{f_{\mathrm{DPS}} \times \sigma_{J/\psi J/\psi}},$$
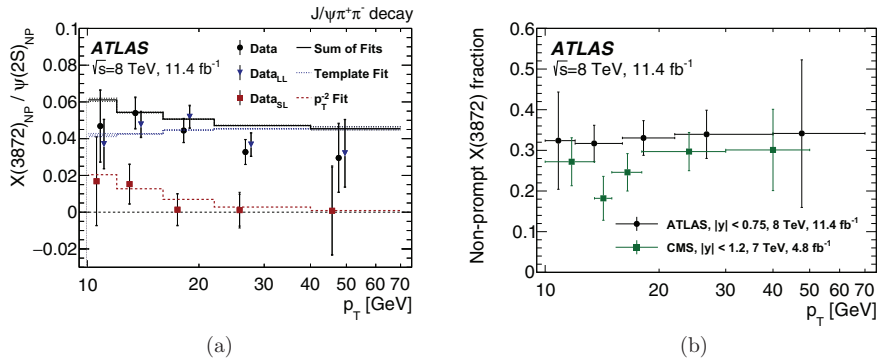
(a)

(b)

Fig. 2. – (a) Ratio of cross sections times branching fractions, $X(3872)/\psi(2S)$, for non-prompt production, in the two-lifetime fit model. The total non-prompt ratio (black circles) is separated into short-lived (red squares) and long-lived (blue triangles) components for the $X(3872)$. (b) Measured non-prompt fractions for $X(3872)$ production, compared to CMS results at $\sqrt{s} = 7$ TeV.
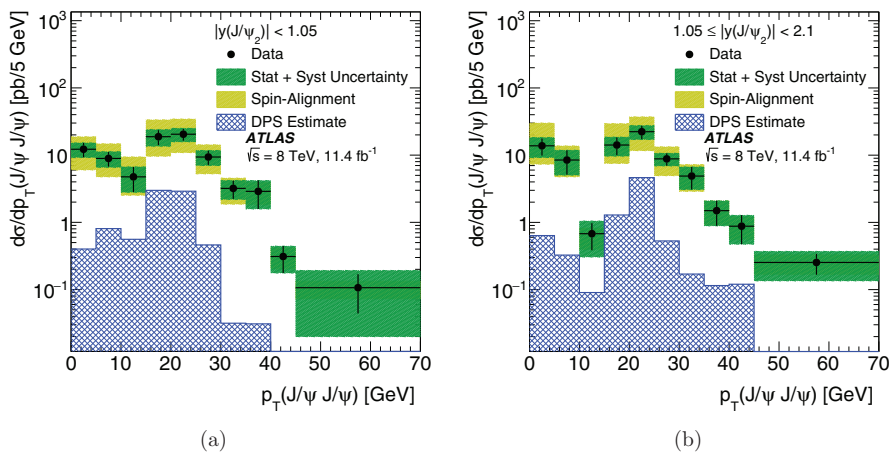

(a)

(b)

Fig. 3. – The differential cross-section, $\mathrm{d}\sigma/\mathrm{d}p_{\mathrm{T}}(J/\psi J/\psi)$, in the (a) central and (b) forward rapidity. The variation due to the choice of J/ψ spin-alignment is shown separately. Also shown is the data-driven DPS distribution. The two peaks at low and high p_{T} are due to the away and towards event topologies, respectively. The separation is due to the requirement that each J/ψ have $p_{\mathrm{T}} > 8.5$ GeV.

where f_{DPS} is the fraction of prompt–prompt (PP) di-J/ψ events that are due to DPS. The factor of $1/2$ is because the two final states for di-J/ψ events are identical.

The production of two prompt J/ψ mesons [13] is studied using a sample of proton-proton collisions at $\sqrt{s} = 8$ TeV, corresponding to an integrated luminosity of $11.4\,\mathrm{fb}^{-1}$ collected in 2012 with the ATLAS detector at the LHC. The J/ψ candidates are selected with transverse momentum $p_{\mathrm{T}} > 8.5$ GeV and rapidity $|y| < 2.1$. The main sources of background to PP di-J/ψ production are studied and subtracted from the observed data, including the non-J/ψ events, non-prompt J/ψ events, and pile-up background. The PP di-J/ψ signal is extracted by doing a two-dimensional fit of the decay length distribution of the leading J/ψ meson against the sub-leading J/ψ distribution.
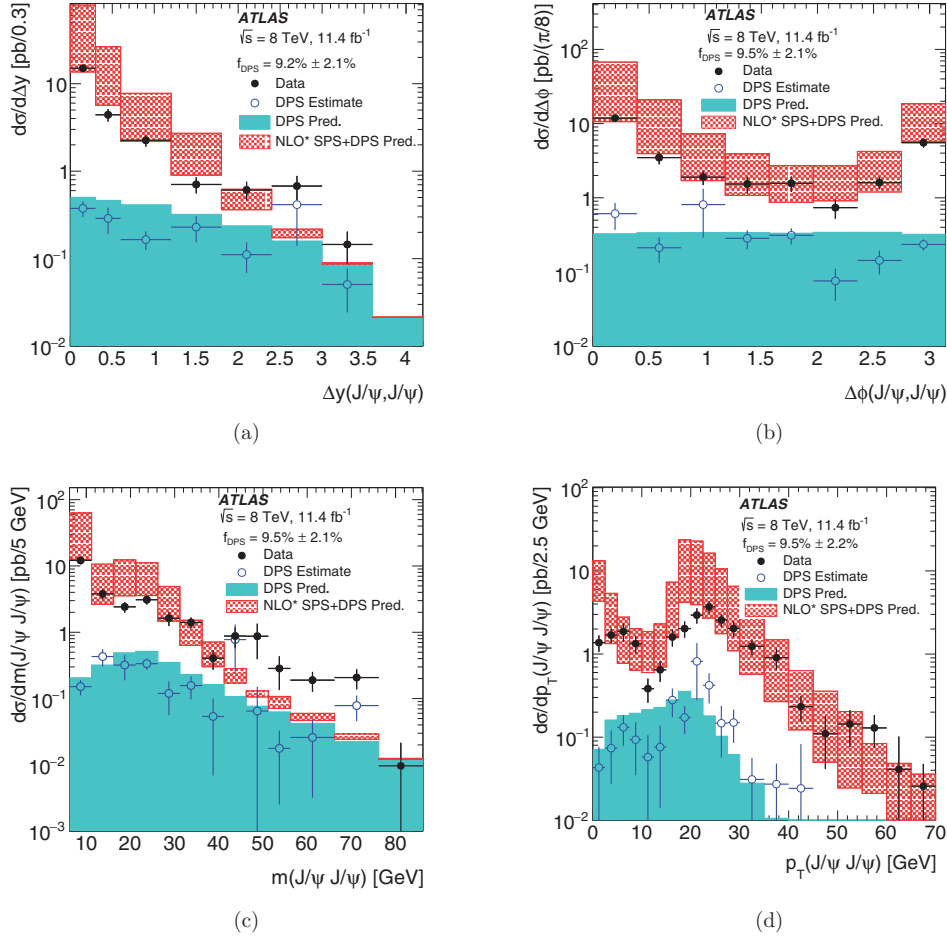
Fig. 4. – The DPS and total differential cross-sections as a function of (a) the difference in rapidity between the two J/ψ mesons, (b) the azimuthal angle between the two J/ψ mesons, (c) the invariant mass of the di-J/ψ, (d) the transverse momentum of the di-J/ψ. Shown are the data as well as the LO DPS [14] + NLO* SPS [15, 16] predictions. The DPS predictions are normalised to the value of f_{DPS} found in the data and the NLO* SPS predictions are multiplied by a constant feed-down correction factor. The data-driven DPS-weighted distribution and the total data distribution are compared to the DPS theory prediction and the total SPS + DPS prediction.

The differential cross-sections as a function of $p_T(J/\psi J/\psi)$ and $m(J/\psi J/\psi)$ are shown in fig. 3. There are two peaks in the di-J/ψ p_T distribution. The peak near zero is due to events in which the J/ψ are produced back-to-back in an *away* topology and the peak at higher p_T is due to events that have a *towards* topology in which the two J/ψ are produced in the same direction and are back-to-back with respect to an additional gluon.

A data-driven approach is used to extract the DPS contribution, in order to minimise the dependence on theoretical predictions. The DPS sample is simulated by combining re-sampled J/ψ mesons from two different random events in the selected di-J/ψ sample.
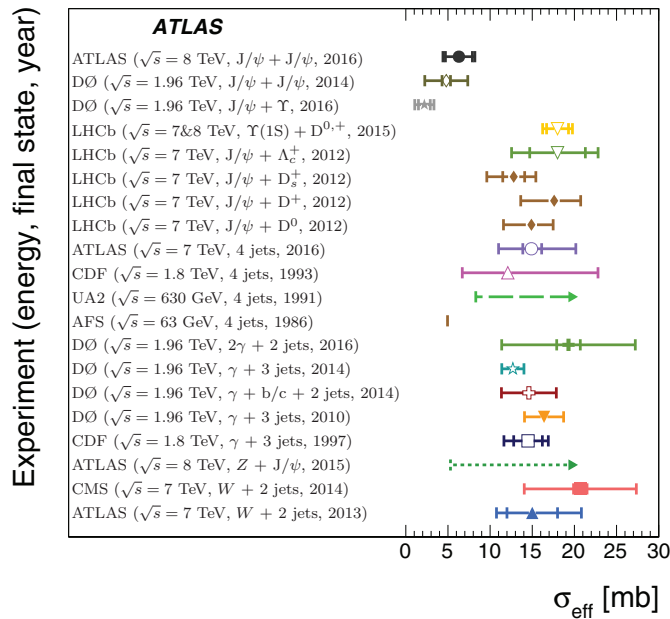
Fig. 5. – The effective cross-section of DPS from different energies and final states measured by the AFS experiment [17], the UA2 experiment [18], the CDF experiment [19, 20], the D0 experiment [21-25], the CMS experiment [26], the LHCb experiment [27, 28], and the ATLAS experiment [29-31]. The inner error bars represent the statistical uncertainties and the outer error bars represent the sum in quadrature of the statistical and systematic uncertainties. Dashed arrows indicate lower limits and the vertical line represents the AFS measurement published without uncertainties.

Then the DPS contribution is normalised to a DPS enriched region with $\Delta y \geq 1.8$ and $\Delta\phi \leq \pi/2$. The measured DPS-weighted distributions are compared to the LO DPS [14] + NLO SPS [15,16] predictions, as shown in fig. 4. The shape of the data-driven DPS distribution approximately agrees with the shape of the DPS predictions. However, there is disagreement between the total data distribution and the total theory predictions at large Δy, large invariant mass, and in the low-p_{T} region that corresponds to di-J/ψ production in an away topology. Significant fraction of towards topology where the NLO SPS contributions dominate is observed, specifically events in the low-$\Delta\phi$ region of fig. 4(b) and the peak of the di-J/ψ p_{T} distribution in fig. 4(d) at around $p_{\mathrm{T}} = 22\,\mathrm{GeV}$. Therefore LO predictions alone, which do not include the towards topology, are not enough to describe PP di-J/ψ production. Using the Δy distribution the fraction of DPS is measured to be: $f_{\mathrm{DPS}} = (9.2 \pm 2.1\,(\mathrm{stat}) \pm 0.5\,(\mathrm{syst}))\%$.

Finally, the effective cross-section for prompt J/ψ meson pair production at $\sqrt{s} = 8\,\mathrm{TeV}$ is measured to be $\sigma_{\mathrm{eff}} = 6.3 \pm 1.6\,(\mathrm{stat}) \pm 1.0\,(\mathrm{syst}) \pm 0.1\,(\mathrm{BF}) \pm 0.1\,(\mathrm{lumi})\,\mathrm{mb}$. The effective cross-section measured in this analysis is compared to measurements from other experiments and processes in fig. 5. The ATLAS data suggest that the effective cross-section measured from the prompt di-J/ψ final state could be lower than that measured for the other final states. However, the latest prompt di-J/ψ measurement from LHCb [32] at 13 TeV shows a higher measured effective cross-section. Further studies with increased luminosity at the LHC is desired to understand those measurements.

4. – Summary

Latest results on production of quarkonia states with the ATLAS detector are presented, based on data collected at 8 TeV. For $X(3872)$ production measurement, an enhancement in the non-prompt production at low p_{T}, and of a shorter effective lifetime, is observed. The enhancement might be related to production of the B_c state that decays inclusively to $X(3872)$. The differential $J/\psi + J/\psi$ cross-section is measured and the fraction of prompt pair events due to double parton scattering is determined by studying kinematic correlations. The effective cross-section is measured and compared to measurements from other experiments and processes. Further studies with increased luminosity at 13 TeV are desired to understand the features observed.

REFERENCES

[1] BELLE COLLABORATION (CHOI S. K. *et al.*), *Phys. Rev. Lett.*, **91** (2003) 262001, arXiv:hep-ex/0309032.
[2] BABAR COLLABORATION (AUBERT B. *et al.*), *Phys. Rev. D*, **71** (2005) 071103, arXiv:hep-ex/0406022.
[3] D0 COLLABORATION (ABAZOV V. M. *et al.*), *Phys. Rev. Lett.*, **93** (2004) 162002, arXiv:hep-ex/0405004.
[4] LHCb COLLABORATION (AAIJ R. *et al.*), *Eur. Phys. J. C*, **72** (2012) 1972, arXiv:1112.5310 [hep-ex].
[5] PARTICLE DATA GROUP (OLIVE K. A. *et al.*), *Chin. Phys. C*, **38** (2014) 090001.
[6] TOMARADZE A., DOBBS S., XIAO T. and SETH K. K., *Phys. Rev. D*, **91** (2015) 011102, arXiv:1501.01658 [hep-ex].
[7] CMS COLLABORATION (CHATRCHYAN S. *et al.*), *JHEP*, **04** (2013) 154, arXiv:1302.3968 [hep-ex].
[8] MENG C., HAN H. and CHAO K. T., arXiv:1304.6710 [hep-ph].
[9] ATLAS COLLABORATION (AABOUD M. *et al.*), *JHEP*, **01** (2017) 117, arXiv:1610.09303 [hep-ex].
[10] CACCIARI M., FRIXIONE S., HOUDEAU N., MANGANO M. L., NASON P. and RIDOLFI G., *JHEP*, **10** (2012) 137, arXiv:1205.6344 [hep-ph].
[11] ARTOISENET P. and BRAATEN E., *Phys. Rev. D*, **81** (2010) 114018, arXiv:0911.2016 [hep-ph].
[12] HUMPERT B., *Phys. Lett. B*, **131** (1983) 461.
[13] ATLAS COLLABORATION (AABOUD M. *et al.*), *Eur. Phys. J. C*, **77** (2017) 76, arXiv:1612.02950 [hep-ex].
[14] BORSCHENSKY C. and KULESZA A., *Phys. Rev. D*, **95** (2017) 034029, arXiv:1610.00666 [hep-ph].
[15] LANSBERG J. P. and SHAO H. S., *Phys. Lett. B*, **751** (2015) 479, arXiv:1410.8822 [hep-ph].
[16] LANSBERG J. P. and SHAO H. S., *Phys. Rev. Lett.*, **111** (2013) 122001, arXiv:1308.0474 [hep-ph].
[17] AXIAL FIELD SPECTROMETER COLLABORATION (AKESSON T. *et al.*), *Z. Phys. C*, **34** (1987) 163.
[18] UA2 COLLABORATION (ALITTI J. *et al.*), *Phys. Lett. B*, **268** (1991) 145.
[19] CDF COLLABORATION (ABE F. *et al.*), *Phys. Rev. D*, **47** (1993) 4857.
[20] CDF COLLABORATION (ABE F. *et al.*), *Phys. Rev. Lett.*, **79** (1997) 584.
[21] D0 COLLABORATION (ABAZOV V. M. *et al.*), *Phys. Rev. D*, **81** (2010) 052012, arXiv:0912.5104 [hep-ex].
[22] D0 COLLABORATION (ABAZOV V. M. *et al.*), *Phys. Rev. D*, **89** (2014) 072006, arXiv:1402.1550 [hep-ex].
[23] D0 COLLABORATION (ABAZOV V. M. *et al.*), *Phys. Rev. D*, **90** (2014) 111101, arXiv:1406.2380 [hep-ex].

[24] D0 COLLABORATION (ABAZOV V. M. *et al.*), *Phys. Rev. Lett.*, **116** (2016) 082002, arXiv:1511.02428 [hep-ex].

[25] D0 COLLABORATION (ABAZOV V. M. *et al.*), *Phys. Rev. D*, **93** (2016) 052008, arXiv:1512.05291 [hep-ex].

[26] CMS COLLABORATION (CHATRCHYAN S. *et al.*), *JHEP*, **03** (2014) 032, arXiv:1312.5729 [hep-ex].

[27] LHCb COLLABORATION (AAIJ R. *et al.*), *JHEP*, **06** (2012) 141; **03** (2014) 108(Addendum), arXiv:1205.0975 [hep-ex].

[28] LHCb COLLABORATION (AAIJ R. *et al.*), *JHEP*, **07** (2016) 052, arXiv:1510.05949 [hep-ex].

[29] ATLAS COLLABORATION (AAD G. *et al.*), *New J. Phys.*, **15** (2013) 033038, arXiv:1301.6872 [hep-ex].

[30] ATLAS COLLABORATION (AAD G. *et al.*), *Eur. Phys. J. C*, **75** (2015) 229, arXiv:1412.6428 [hep-ex].

[31] ATLAS COLLABORATION (AABOUD M. *et al.*), *JHEP*, **11** (2016) 110, arXiv:1608.01857 [hep-ex].

[32] LHCb COLLABORATION (AAIJ R. *et al.*), arXiv:1612.07451 [hep-ex].